ACS Energy Letters

http://pubs.acs.org/journal/aelccp

LETTER

Defect Passivation of Organic−Inorganic Hybrid Perovskites by Diammonium Iodide toward High-Performance Photovoltaic Devices

Ting Zhao,[†] Chu-Chen Chueh,[†] Qi Chen,[†] Adharsh Rajagopal,[†] and Alex K.-Y. Jen*[,†,‡]

[†]Department of Materials Science and Engineering and [‡]Department of Chemistry, University of Washington, Seattle, Washington 98195, United States

Supporting Information

ABSTRACT: The polycrystalline feature of solution-processed perovskite film and its ionic nature inevitably incur substantial crystallographic defects, especially at the film surface and the grain boundaries (GBs). Here, a simple defect passivation method was exploited by post-treating $CH_3NH_3PbI_3$ ($MAPbI_3$) film with a rationally selected diammonium iodide. The molecular structure of the used diammonium iodide was discovered to play a critical role in affecting the phase purity of treated $MAPbI_3$. Both $NH_3I(CH_2)_4NH_3I$ and $NH_3I(CH_2)_2O(CH_2)_2NH_3I$ (EDBE) induce three-dimensional (3D) to two-dimensional (2D) perovskite phase transformation during the treatment while only $NH_3I(CH_2)_8NH_3I$ (C8) successfully passivates perovskite surface and GBs without forming 2D perovskite because of the elevated activation energy arising from its unique anti−gauche isomerization. Defect passivation of $MAPbI_3$ was clearly confirmed by scanning Kelvin probe microscopy (SKPM) and time-resolved photoluminescence (TRPL) studies, which results in the reduced recombination loss in derived devices. Consequently, the perovskite solar cell with C8 passivation showed a much improved power conversion efficiency (PCE) of 17.60% compared to the control device PCE of 14.64%.

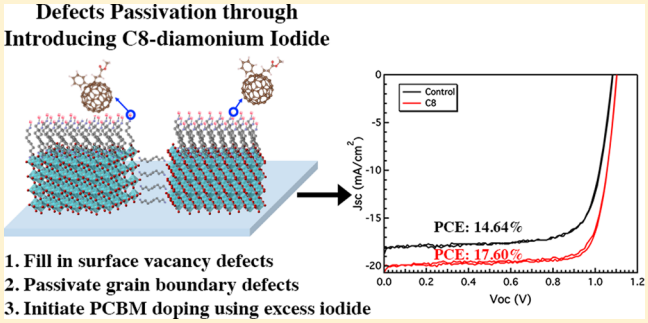

Organometal trihalide perovskites (OTPs) have undergone a rapid development as promising photovoltaic materials with power conversion efficiencies (PCEs) increasing from 3.8% to 22% within just a few years.[1−4] Besides high absorption coefficient, ambipolar charge transport, high charge carrier mobility, and long electron−hole diffusion lengths,[5−9] OTPs' compatibility with simple low-temperature solution processes provides great promise for future commercialization.[10] However, a consequence of solution processing is the polycrystallinity of prepared thin films, which results in substantial structural disorder and crystallographic defects.[11,12] Several reports have identified the prevalence of vacancy and interstitial defects in OTP thin films due to their low formation energies.[13−16] In principle, these defects incur trap-assisted nonradiative recombination losses and thus deteriorate the resulting photovoltaic performance. In addition, vacancy defects provide a pathway for ion migration, which adversely affects the charge collection and results in current−voltage hysteresis.[17−20] Therefore, effective mitigation of defects in the solution-processed perovskite films is an important research subject to further enhance the performance of perovskite solar cells (PVSCs) toward their thermodynamic limits.

In an ionic crystal like OTP, dangling bonds at the surface and grain boundaries (GBs) introduce trap states and nonradiative recombination centers. The polycrystalline nature of solution-processed OTP films further aggravates this issue because of increased GB density and structural disorder, in contrast to a single-crystalline perovskite that shows an extremely long electron−hole diffusion length of 175 μm.[21] Several studies have indicated that surface defects and GBs can serve as photoluminescence (PL) quenching sites and thus result in loss of photogenerated carriers.[22−25] Additionally, it has also been reported that ion migration becomes more pronounced in a polycrystalline material, due to higher diffusivity of ions across extended defects like GBs.[26] Thus, it is critical to develop effective methods that can passivate the defects at the film surface and GBs in OTPs.

Recently, several approaches have been reported to be able to passivate the surface/interfaces and GBs of solution-processed OTP films. For example, PbI_2 preferably formed at GBs through high-temperature annealing creates a type I band alignment at GBs, resulting in defect passivation and retardation of carrier recombination.[27−29] Meanwhile, small molecules have also been employed to passivate dangling bonds in OTPs by exploiting the

Received: August 3, 2016
Accepted: September 12, 2016

 © XXXX American Chemical Society

DOI: 10.1021/acsenergylett.6b00327
ACS Energy Lett. 2016, 1, 757−763

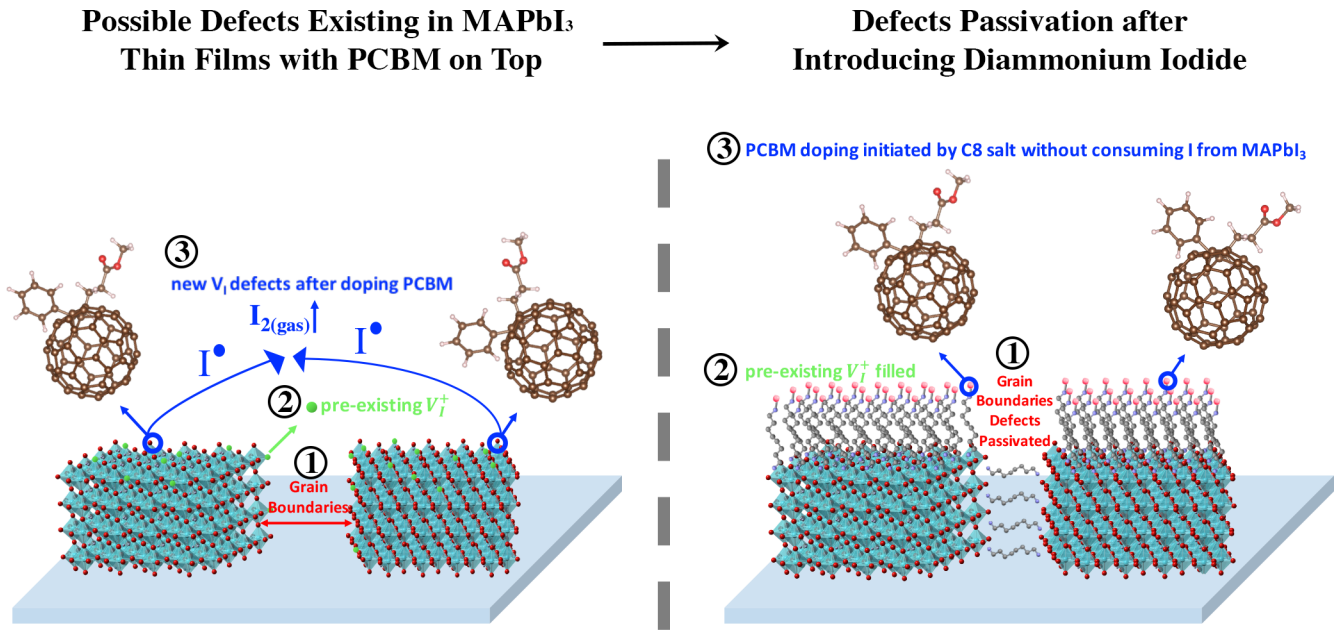

Figure 1. Summary scheme for (left panel) possible defects existing in $MAPbI_3$ thin films with PCBM on top as electron transport layer and (right panel) defects passivation mechanism after introducing diammonium iodide through post treatment.

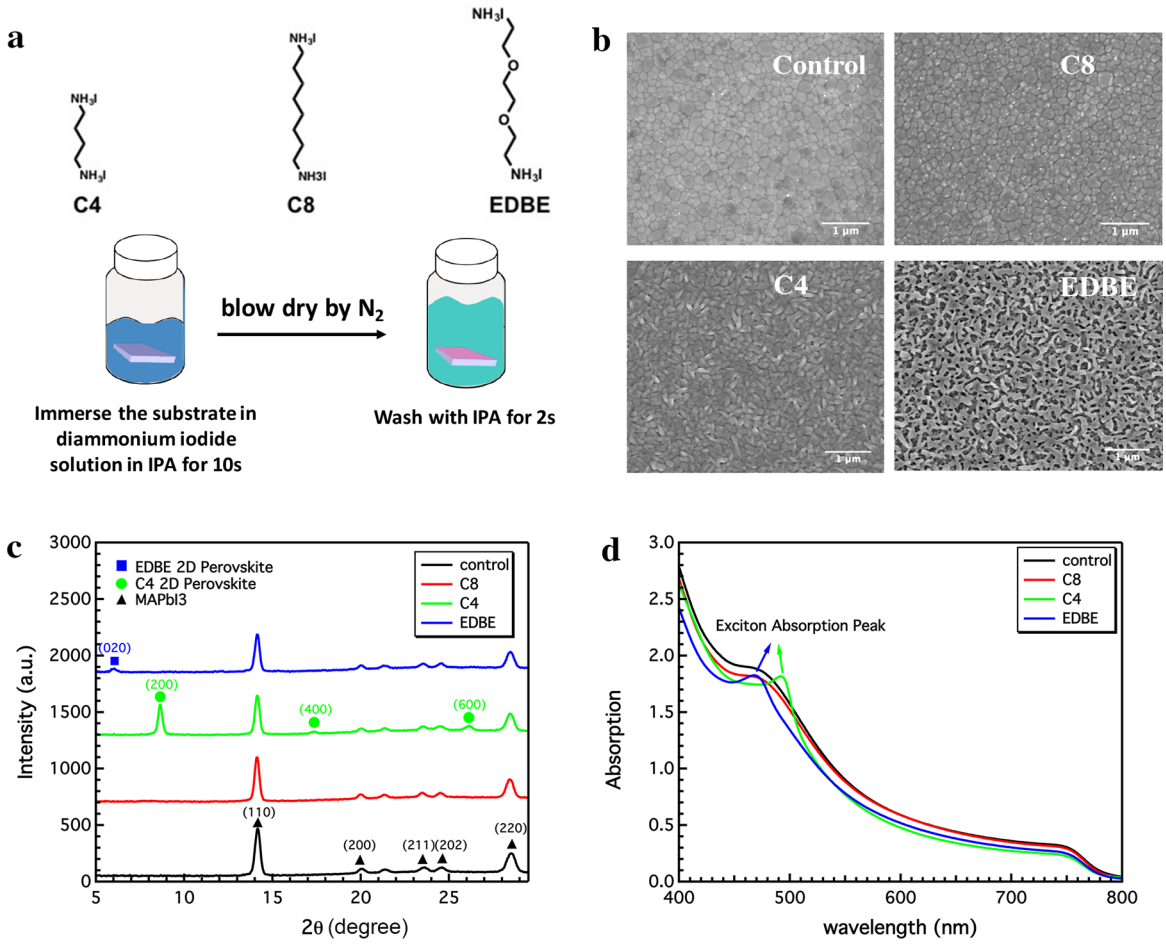

Figure 2. (a) Three kinds of diammonium iodide salts (abbreviated C4, C8, and EDBE) selected for perovskite passivation and the processing details. (b) SEM images where the scale bar corresponds to 1 μm. (c) XRD and (d) UV-absorption of control film ($MAPbI_3$) and C8-, C4-, and EDBE-treated films.

DOI: 10.1021/acsenergylett.6b00327
ACS Energy Lett. 2016, 1, 757−763

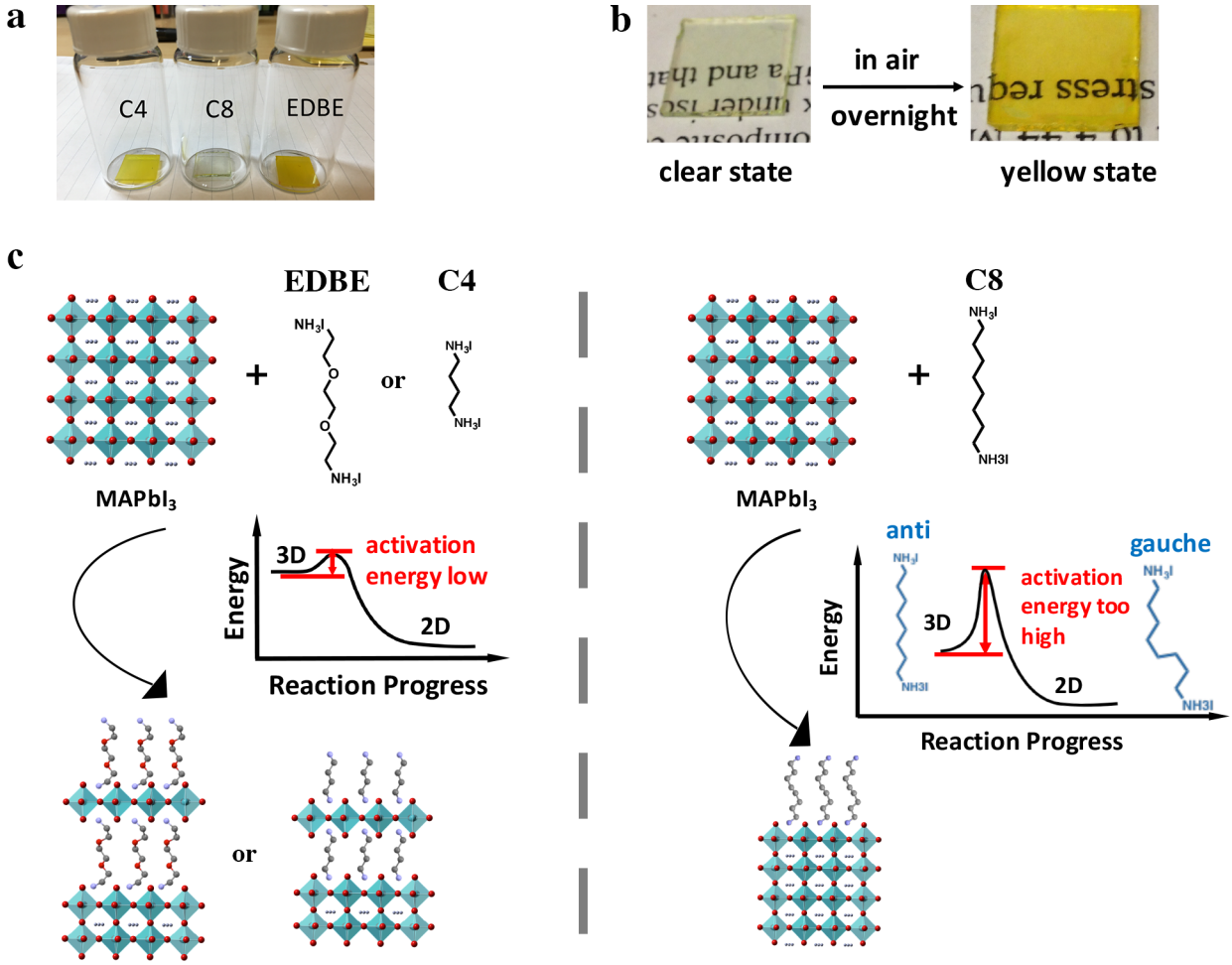

Figure 3. (a) Photos of C4-, C8-, and EDBE-PbI_4 thin films after the spin-coating and annealing process as illustrated in the Supporting Information. (b) Photo of C8−PbI_4 thin film transferring from clear state to yellow state after being put in air overnight. (c) Schematic demonstration of why EDBE and C4 treatment can induce respective 2D hybrid perovskite formation, while C8 stays only at the surface or grain boundaries without affecting bulk properties.

associated intermolecular interaction.[30−32] Lately, we and several groups have discovered that the commonly used fullerene-based electron-transporting layers (ETLs) can also passivate surface trap states and GB defects in OTPs to eliminate trap states and suppress device hysteresis.[33−35]

However, the role of fullerene in eliminating the dominant vacancy defects is limited. We and several groups have found that iodide in perovskites has the propensity to dope fullerene at the perovskite/fullerene interface.[33,36,37] In this case, iodo radicals would be inevitably generated after doping and then form iodine that can potentially sublime easily. As a result, new V_I defects can possibly be generated inside the perovskite film. Thus, for fullerene-based inverted PVSCs, it would be ideal if the perovskite surface and GBs can be passivated without generating new defects due to perovskite fullerene interaction.

In this study, a series of diammonium iodides, namely, C4, C8, and EDBE, were explored to passivate perovskite surface and GBs considering their bilateral ammonium iodide end can simultaneously passivatethe perovskite layer and dope the adjacent electron-transporting layer (PCBM herein) in derived PVSCs, as illustrated in Figure 1. In pursuing the suitable materials for defect passivation, we surprisingly discovered that the molecular structure of diammonium iodide plays a critical role in affecting perovskite's surface morphology and phase purity. We found that both C4 and EDBE can induce three-dimensional (3D) to two-dimensional (2D) perovskite phase transformation during post treatment. However, the activation energy for such transition can be modulated by tailoring the molecular structure of the diammonium iodides. The C8 can successfully passivate perovskite surface and GBs without causing 2D phase transformation of $CH_3NH_3PbI_3$ because of its unique anti−gauche isomerization, which may elevate the activation energy for the 3D-to-2D phase transformation. Consequently, the thin-film PVSC passivated by C8 shows a much improved power conversion efficiency (PCE) of 17.60% compared to 14.64% for the control device.

Diammonium Iodides for Perovskite Passivation. To effectively passivate the above-mentioned defects, three diammounium iodides with different molecular structures, C4, C8, and EDBE (Figure 2a), were selected because their bilateral ammonium iodide group is capable of simultaneously passivating perovskite surface/GBs and inducing PCBM doping without consuming iodides from bulk perovskite (Figure 1). We first try to investigate the effect of alkyl chain length on electron transfer from perovskite to PCBM by comparing C4 and C8. The EDBE is included in our exploration to study whether the hydrogen bonding between adjacent EDBE molecules[38] will influence the self-assembly kinetics between the organic species and perovskite for better passivation effects.

DOI: 10.1021/acsenergylett.6b00327
ACS Energy Lett. 2016, 1, 757−763

The post-treatment procedure is illustrated in Figure 2a and detailed in the Supporting Information. It is important to note that similar surface topology and bulk properties such as crystallinity and absorption coefficient of perovskite films should be retained if the diammonium iodide distributes only at the perovskite surface or in the GBs. To examine this, the evolution of surface morphology of post-treatment perovskite films is investigated by scanning electron microscopy (SEM) (Figure 2b). As clearly shown, only the C8-treated film showed surface morphology similar to that of the pristine film, which encompasses a compact and uniform film with grain sizes ranging from tens of nanometers to around 200 nm. However, the C4- and EDBE-treated films showed distinct morphology with striplike and branchlike features, respectively.

The enormous change in surface morphology of C4- and EDBE-treated films prompt us to speculate the possibility of 3D-to-2D perovskite phase transformation due to the tendency of large-sized diammonium iodides to form 2D hybrid perovskites,[38,39] which induce the morphological changes through dissolution−recrystallization.[40] To probe this, X-ray diffraction (XRD) and ultraviolet−visible (UV−vis) absorption of post-treated films were measured to study if the relatively larger organic cations diffuse into the pristine perovskite film and partially convert the perovskite from 3D to 2D.

As clearly evidenced from the XRD data shown in Figure 2c, the characteristic diffraction corresponding to {200} planes of (C4)PbI_4 and (020) plane of (EDBE)PbI_4 are apparent in the C4- and EDBE-treated films, respectively. In addition, their corresponding UV−vis absorption spectra (Figure 2d) clearly show the excitonic absorption peak, affirming the formation of 2D perovskite due to the intercalation of C4 and EDBE cations into the perovskite films. However, the C8-treated film seems to uniquely preserve its morphology and phase purity without going through such transition (Figure 2b−d).

The 3D-to-2D perovskite phase transformation induced by C4 and EDBE cations can be explained by the tendency of forming more thermodynamically stable 2D hybrid perovskite.[41−44] The reaction rate for such 3D-to-2D phase transformation is in principle determined by its associated activation energy. Therefore, the inhibited phase transformation observed in C8-treated films might be due to two possible reasons: (i) The phase transformation from 3D $MAPbI_3$ to 2D (C8)PbI_4 occurs too slowly to be effectively observed during the fast 10 s treatment period. (ii) The (C8)PbI_4 in nature has a higher Gibbs free energy than $MAPbI_3$.

The distinction in morphological variation between C4/EDBE- and C8-treated films further triggered us to ponder the structural difference of their corresponding 2D perovskites. Interestingly, Lemmerer and Billing[39] found that, among all of their studied 2D lead-halide-based perovskites incorporating diammonium cations, C8 is the only material that has gauche conformation in the middle of the alkyl chain while other diammomium cations consist of only the anti conformation. This gauche conformation has higher energy compared to the anti conformation, and the associated local energy minimum is metastable. Thus, it can be inferred that the middle part of the C8 diammonium cation needs to convert from its energetically stable anti form into the gauche conformation to intercalate into the 2D perovskite film. Such anti−gauche isomerization necessitates additional energy barrier for 3D-to-2D phase transformation, thereby slowing the conversion.

To prove this hypothesis, the 2D hybrid perovskite ($n = 1$) thin films based on C4, C8, and EDBE were prepared accordingly

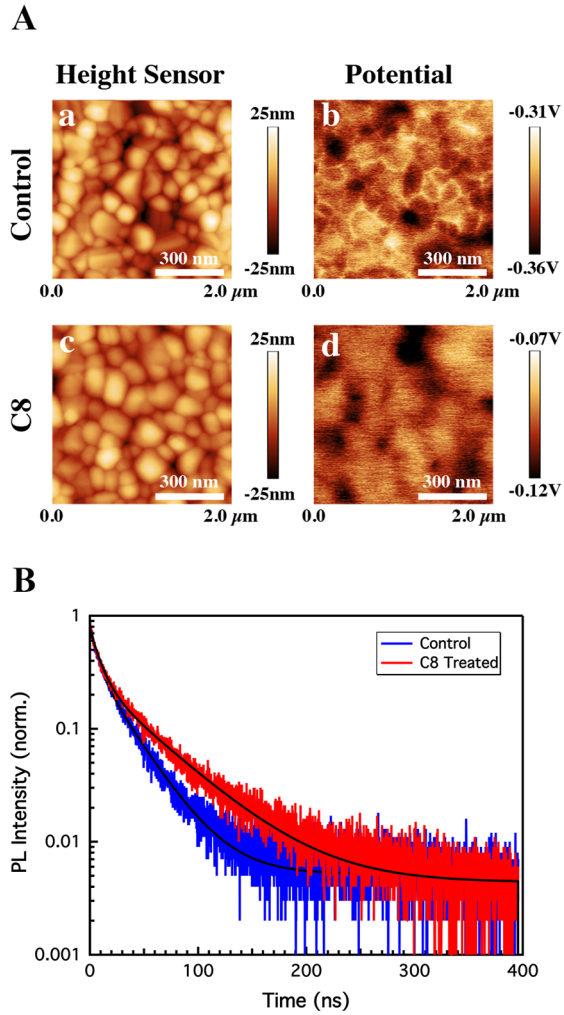

Figure 4. (A) 2D topology (a, c) and surface potential maps (b, d) for control and C8-treated perovskite films. (B) PL decay for control and C8-treated films on glass.

by a simple spin-coating procedure (Supporting Information). As shown in Figure 3a, both spin-coated C4 and EDBE films convert immediately into a yellow color after being placed onto the preheated (100 °C) hot plate, whereas the C8 film remains clear after being annealed at 100 °C for 10 min. As previously reported by Lemmerer and Billing,[39] the single crystal of C8−PbI_4 possesses a yellow color as well, which is typical for lead-iodide-based 2D hybrid perovskites. Therefore, we can conclude that the elevated activation energy for forming the corresponding 2D C8−PbI_4 perovskite phase is the reason for forming the clear intermediate state (Figure 3c; will be discussed later). Interestingly, it was discovered that exposing the C8 films in air facilitates the 2D phase transformation. As shown in Figure 3b, the C8 film turns into a yellow color after being stored in air overnight. Its corresponding XRD and UV−vis absorption results are presented in Figure S1, where the yellow phase is clearly identified to be the 2D C8−PbI_4. However, the C8 film remains in the clear state even after being stored in N_2 for a week. This result suggests that moisture or/and oxygen play a critical role in lowering the activation energy for this phase transformation, and the exact mechanism is still under investigation.

Because the 2D C8−PbI_4 film can be eventually formed (Figure 3b) and is quite stable in air, we hypothesize that although anti−gauche isomerization may also raise the 2D

DOI: 10.1021/acsenergylett.6b00327
ACS Energy Lett. 2016, 1, 757−763

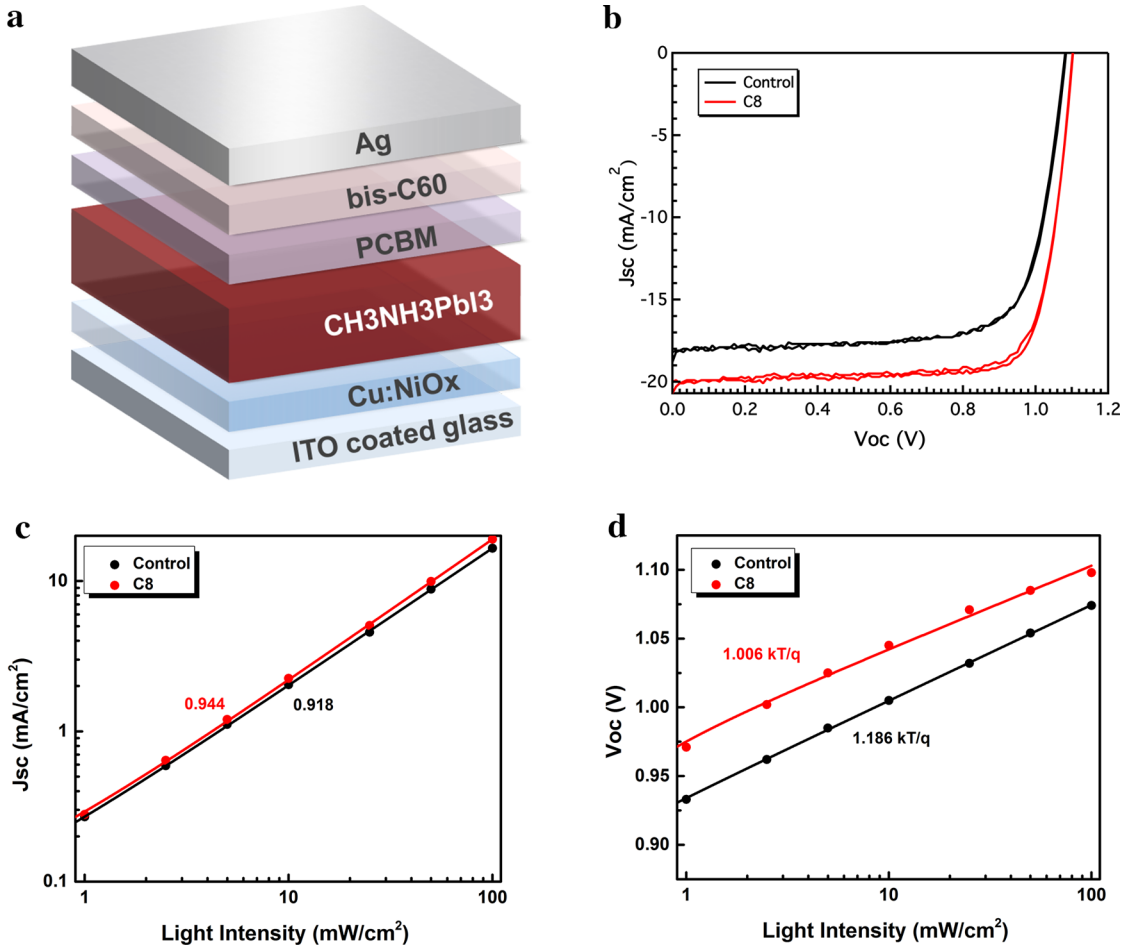

Figure 5. (a) Device architecture used in this study. (b) J−V characteristics of control and C8-treated devices. Dependence of (c) J_{SC} and (d) V_{OC} on light intensity.

C8−PbI_4 phase's Gibbs free energy, it is still lower than that of the 3D $MAPbI_3$ phase. Hence, the change in Gibbs free energy should play a less important role than the elevation of activation energy in mediating 3D-to-2D perovskite phase transformation in C8 post treatment. A scheme showing the reaction mechanism of the studied diammonium salts is illustrated in Figure 3c. Our results reveal that owing to the higher thermodynamic stability of 2D perovskites, most organic salts with larger cations used for perovskite passivation will induce fast 3D-to-2D phase transformation (within 10 s) due to the low activation energy of this process. However, the extra anti−gauche isomerization energy for C8 slows the self-assembling process and thus limits itself to be distributed only at the perovskite surface and GBs.

Defect Passivation Characterization. After elucidating that only C8 can successfully interact with pristine perovskite without affecting its bulk properties, we next examined its efficacy in defect passivation. Scanning Kelvin probe microscopy (SKPM)[45,46] is employed to investigate the perovskite films before and after C8 treatment. Figure 4A illustrates the topography (left column) and surface potential (SP) (right column) images of the perovskite films before (top row) and after (bottom row) treatment. The root-mean-square (RMS) roughness of perovskite films before and after treatment are 7.99 and 5.99 nm, respectively. As can be clearly seen, both films showed similar morphology, affirming no surface reconstruction of perovskite film after C8 treatment, which is consistent with the SEM image shown in Figure 2b. Notably, the small decrease in surface roughness of the treated film indicates that C8 did fill in the GBs and thus reduces the height difference between the grain surface and GB.

Despite the similarity in surface morphology, the two films showed distinctly different SP. For the control film without treatment, most GBs showed SP higher than that of the interior grains, indicating a downward band-bending in the GBs which will cause electron trapping.[25,27] However, the SP difference between GBs and interior grains is significantly reduced after treatment, indicating negligible band bending at this corresponding interface. This will facilitate electron transport across the GBs. It clearly validates effective perovskite passivation. In addition, the average SP of the treated film (−0.10 V) shows an increase of 0.24 V compared to that of pristine film (−0.34 V). This suggests a larger downward surface band-bending of the treated film, which can benefit charge carrier separation and facilitate the electron collection toward ETL in derived devices.[47]

Time-resolved photoluminescence (TRPL) has also been utilized to further examine the effects of defect passivation on resulting photophysical properties, as shown in Figure 4B. The average lifetime of perovskite film increased from 24 to 40 ns after C8-treatment with both improved fast and slow component, revealing the suppressed charge recombination in the treated film. The fitting and detailed parameters are summarized in Table S1.

DOI: 10.1021/acsenergylett.6b00327
ACS Energy Lett. 2016, 1, 757−763

Photovoltaic Performance Characterization and Recombination Kinetics Study. To examine how C8-passivation affects the photovoltaic properties, planar heterojunction structure (PHJ) devices were fabricated in the configuration shown in Figure 5a. The detailed fabrication procedure is described in the Supporting Information, and the statistical device performance with standard deviation for control and C8-, C4-, and EDBE-treated devices is shown in Table S2. As expected, the PCE of the derived PVSC is significantly improved from 14.64% to 17.60% after C8-treatment (Figure 5b) with a marked increase in all photovoltaic parameters (Table S2). The steady-state current output of both devices is shown in Figure S2, and it matches well with our measured PCEs. Different from the C8-treated device, the C4- and EDBE-treated PVSCs showed inferior PCEs with a much lower short-circuit current (J_{SC}) and fill factor (FF). This can be attributed to the formation of bulk 2D perovskite, in which the intercalated insulating alkyl chains block electron transfer from perovskite to PCBM and thus impede efficient charge collection.

To better understand the charge carrier dynamics and enhanced performance, we have studied the device recombination kinetics by measuring the dependence of $J-V$ characteristics on light intensity.[48] Figure 5c shows the dependence of J_{SC} on light intensity of the studied devices, in which the fitted slope (in accordance to power law) is 0.918 and 0.944 for the control device and C8-treated device, respectively. This result clearly indicates that the reduced charge recombination loss for the C8-treated device is due to effective defect passivation. Figure 5d shows the relationship between open-circuit voltage (V_{OC}) and light intensity of the studied devices. Notably, the control device possesses a slope of 1.186 kT/q throughout the entire range of light intensity, showing a bimolecular recombination dominant kinetics. This supports the respectable high PCE of the control device. Nevertheless, the C8-treated PVSC showed a further reduced slope of 1.006 kT/q, suggesting a minimized trap-assisted recombination in the device. In addition to the effective defect passivation, this significantly reduced recombination loss can also be attributed to the interfacial doping at the C8/PCBM interface.[33,34,49] The other end of C8 ammonium iodide can dope PCBM without the need of creating further V_I defects inside the perovskite film, leading to a much improved device performance.

In summary, we have successfully developed a simple and effective method to passivate the surface and GB defects of $CH_3NH_3PbI_3$ films by employing alkyl diammonium iodide. It was discovered that the molecular structure of used diammonium salt has a profound effect on influencing the surface morphology and phase purity of perovskite. Both C4- and EDBE-diammonium salts induce 3D-to-2D hybrid perovskite phase transformation during treatment, which is unfavorable for charge transport and device performance because of their insulating nature. However, the 3D-to-2D transition is inhibited in C8-treated films because of its unique anti−gauche isomerization, which elevates the activation energy of this transition. Therefore, the C8 diammonium iodide treatment can successfully passivate perovskite films as evidenced by the SKPM and TRPL measurements. Further investigations on device recombination kinetics also showed reduced charge recombination loss in the derived device, indicating that the C8 salt can also potentially dope PCBM. As a result, the C8-treated PVSC shows a much-improved PCE of 17.60% compared to that of the control device (PCE of 14.64%). This study highlights the importance of rational molecular design for perovskite surface modification and passivation.

■ ASSOCIATED CONTENT

Supporting Information

The Supporting Information is available free of charge on the ACS Publications website at DOI: 10.1021/acsenergylett.6b00327.

Experimental section and additional figures and tables (PDF)

■ AUTHOR INFORMATION

Corresponding Author

*E-mail: ajen@u.washington.edu.

Notes

The authors declare no competing financial interest.

■ ACKNOWLEDGMENTS

This work was supported by the National Science Foundation (DMR-1608279), the Office of Naval Research (N00014-14-1-0246), the Asian Office of Aerospace R&D (FA2386-15-1-4106), and the Department of Energy SunShot (DE-EE 0006710). Q.C. acknowledges Collaborative Academic Training Program for Postdoctoral Fellows support from Collaborative Innovation Center of Suzhou Nano Science and Technology. A.K.-Y.J. thanks the Boeing-Johnson Foundation for financial support. This work was made possible by the Molecular Analysis Facility at the University of Washington.

■ REFERENCES

(1) Kojima, A.; Teshima, K.; Shirai, Y.; Miyasaka, T. Organometal Halide Perovskites as Visible-Light Sensitizers for Photovoltaic Cells. *J. Am. Chem. Soc.* **2009**, *131*, 6050−6051.

(2) Lee, M. M.; Teuscher, J.; Miyasaka, T.; Murakami, T. N.; Snaith, H. J. Efficient Hybrid Solar Cells Based on Meso-Superstructured Organometal Halide Perovskites. *Science (Washington, DC, U. S.)* **2012**, *338*, 643−647.

(3) Jeon, N. J.; Noh, J. H.; Yang, W. S.; Kim, Y. C.; Ryu, S.; Seo, J.; Seok, S. Il. Compositional Engineering of Perovskite Materials for High-Performance Solar Cells. *Nature* **2015**, *517*, 476−480.

(4) Bi, D.; Tress, W.; Dar, M. I.; Gao, P.; Luo, J.; Renevier, C.; Schenk, K.; Abate, A.; Giordano, F.; Correa Baena, J.-P.; et al. Efficient Luminescent Solar Cells Based on Tailored Mixed-Cation Perovskites. *Sci. Adv.* **2016**, *2*, e1501170−e1501170.

(5) Marchioro, A.; Teuscher, J.; Friedrich, D.; Kunst, M.; van de Krol, R.; Moehl, T.; Grätzel, M.; Moser, J.-E. Unravelling the Mechanism of Photoinduced Charge Transfer Processes in Lead Iodide Perovskite Solar Cells. *Nat. Photonics* **2014**, *8*, 250−255.

(6) Heo, J. H.; Im, S. H.; Noh, J. H.; Mandal, T. N.; Lim, C.-S.; Chang, J. A.; Lee, Y. H.; Kim, H.; Sarkar, A.; Nazeeruddin, M. K.; et al. Efficient Inorganic−organic Hybrid Heterojunction Solar Cells Containing Perovskite Compound and Polymeric Hole Conductors. *Nat. Photonics* **2013**, *7*, 486−491.

(7) Green, M. a.; Ho-Baillie, A.; Snaith, H. J. The Emergence of Perovskite Solar Cells. *Nat. Photonics* **2014**, *8*, 506−514.

(8) Stranks, S. D.; Eperon, G. E.; Grancini, G.; Menelaou, C.; Alcocer, M. J. P.; Leijtens, T.; Herz, L. M.; Petrozza, A.; Snaith, H. J. Electron-Hole Diffusion Lengths Exceeding 1 Micrometer in an Organometal Trihalide Perovskite Absorber. *Science* **2013**, *342*, 341−344.

(9) Manser, J. S.; Christians, J. A.; Kamat, P. V. Intriguing Optoelectronic Properties of Metal Halide Perovskites. *Chem. Rev.* **2016**, DOI: 10.1021/acs.chemrev.6b00136.

(10) Williams, S. T.; Rajagopal, A.; Chueh, C. C.; Jen, A. K. Y. Current Challenges and Prospective Research for Upscaling Hybrid Perovskite Photovoltaics. *J. Phys. Chem. Lett.* **2016**, *7*, 811−819.

DOI: 10.1021/acsenergylett.6b00327
ACS Energy Lett. 2016, 1, 757−763

(11) Choi, J. J.; Yang, X.; Norman, Z. M.; Billinge, S. J. L.; Owen, J. S. Structure of Methylammonium Lead Iodide within Mesoporous Titanium Dioxide: Active Material in High-Performance Perovskite Solar Cells. *Nano Lett.* **2014**, *14*, 127−133.

(12) Manser, J. S.; Saidaminov, M. I.; Christians, J. A.; Bakr, O. M.; Kamat, P. V. Making and Breaking of Lead Halide Perovskites. *Acc. Chem. Res.* **2016**, *49* (2), 330−338.

(13) Yin, W.-J.; Shi, T.; Yan, Y. Unusual Defect Physics in $CH_3NH_3PbI_3$ Perovskite Solar Cell Absorber. *Appl. Phys. Lett.* **2014**, *104*, 063903.

(14) Buin, A.; Pietsch, P.; Xu, J.; Voznyy, O.; Ip, A. H.; Comin, R.; Sargent, E. H. Materials Processing Routes to Trap-Free Halide Perovskites. *Nano Lett.* **2014**, *14*, 6281−6286.

(15) Walsh, A.; Scanlon, D. O.; Chen, S.; Gong, X. G.; Wei, S. H. Self-Regulation Mechanism for Charged Point Defects in Hybrid Halide Perovskites. *Angew. Chem., Int. Ed.* **2015**, *54*, 1791−1794.

(16) Kim, J.; Lee, S.-H. H.; Lee, J. H.; Hong, K.-H. H. The Role of Intrinsic Defects in Methylammonium Lead Iodide Perovskite. *J. Phys. Chem. Lett.* **2014**, *5*, 1312−1317.

(17) Snaith, H. J.; Abate, A.; Ball, J. M.; Eperon, G. E.; Leijtens, T.; Noel, N. K.; Stranks, S. D.; Wang, J. T.-W.; Wojciechowski, K.; Zhang, W. Anomalous Hysteresis in Perovskite Solar Cells. *J. Phys. Chem. Lett.* **2014**, *5*, 1511−1515.

(18) Azpiroz, J. M.; Mosconi, E.; Bisquert, J.; De Angelis, F. Defect Migration in Methylammonium Lead Iodide and Its Role in Perovskite Solar Cell Operation. *Energy Environ. Sci.* **2015**, *8*, 2118−2127.

(19) Eames, C.; Frost, J. M.; Barnes, P. R. F.; O'Regan, B. C.; Walsh, A.; Islam, M. S. Ionic Transport in Hybrid Lead Iodide Perovskite Solar Cells. *Nat. Commun.* **2015**, *6*, 7497.

(20) Yuan, Y.; Huang, J. Ion Migration in Organometal Trihalide Perovskite and Its Impact on Photovoltaic Efficiency and Stability. *Acc. Chem. Res.* **2016**, *49*, 286−293.

(21) Dong, Q.; Fang, Y.; Shao, Y.; Mulligan, P.; Qiu, J.; Cao, L.; Huang, J. Electron-Hole Diffusion Lengths > 175 μm in Solution-Grown $CH_3NH_3PbI_3$ Single Crystals. *Science* **2015**, *347*, 967−970.

(22) Tachikawa, T.; Karimata, I.; Kobori, Y. Surface Charge Trapping in Organolead Halide Perovskites Explored by Single-Particle Photoluminescence Imaging. *J. Phys. Chem. Lett.* **2015**, *6*, 3195−3201.

(23) Kong, W.; Ding, T.; Bi, G.; Wu, H. Optical Characterizations of the Surface States in Hybrid Lead−halide Perovskites. *Phys. Chem. Chem. Phys.* **2016**, *18*, 12626−12632.

(24) Peng, W.; Anand, B.; Liu, L.; Sampat, S.; Bearden, B. E.; Malko, A.; Chabal, Y. J. Influence of Growth Temperature on Bulk and Surface Defects in Hybrid Lead Halide Perovskite Films. *Nanoscale* **2016**, *8*, 1627−1634.

(25) de Quilettes, D. W.; Vorpahl, S. M.; Stranks, S. D.; Nagaoka, H.; Eperon, G. E.; Ziffer, M. E.; Snaith, H. J.; Ginger, D. S. Impact of Microstructure on Local Carrier Lifetime in Perovskite Solar Cells. *Science* **2015**, *348*, 683−686.

(26) Shao, Y.; Fang, Y.; Li, T.; Wang, Q.; Dong, Q.; Deng, Y.; Yuan, Y.; Wei, H.; Wang, M.; Gruverman, A.; et al. Grain Boundary Dominated Ion Migration in Polycrystalline Organic−inorganic Halide Perovskite Films. *Energy Environ. Sci.* **2016**, *9*, 1752−1759.

(27) Chen, Q.; Zhou, H.; Song, T.-B.; Luo, S.; Hong, Z.; Duan, H.-S.; Dou, L.; Liu, Y.; Yang, Y. Controllable Self-Induced Passivation of Hybrid Lead Iodide Perovskites toward High Performance Solar Cells. *Nano Lett.* **2014**, *14*, 4158−4163.

(28) Supasai, T.; Rujisamphan, N.; Ullrich, K.; Chemseddine, A.; Chemseddine, Th. Formation of a Passivating $CH_3NH_3PbI_3/PbI_2$ Interface during Moderate Heating of $CH_3NH_3PbI_3$ Layers. *Appl. Phys. Lett.* **2013**, *103*, 183906.

(29) Wang, L.; McCleese, C.; Kovalsky, A.; Zhao, Y.; Burda, C. Femtosecond Time-Resolved Transient Absorption Spectroscopy of CH 3 NH 3 PbI 3 Perovskite Films: Evidence for Passivation Effect of PbI 2. *J. Am. Chem. Soc.* **2014**, *136*, 12205−12208.

(30) Abate, A.; Saliba, M.; Hollman, D. J.; Stranks, S. D.; Wojciechowski, K.; Avolio, R.; Grancini, G.; Petrozza, A.; Snaith, H. J. Supramolecular Halogen Bond Passivation of Organic-Inorganic Halide Perovskite Solar Cells. *Nano Lett.* **2014**, *14*, 3247−3254.

(31) Noel, N. K.; Abate, A.; Stranks, S. D.; Parrott, E. S.; Burlakov, V. M.; Goriely, A.; Snaith, H. J. Enhanced Photoluminescence and Solar Cell Performance via Lewis Base Passivation of Organic−Inorganic Lead Halide Perovskites. *ACS Nano* **2014**, *8*, 9815−9821.

(32) Zhang, J.; Wang, P.; Huang, X.; Xu, J.; Wang, L.; Yue, G.; Lu, X.; Liu, J.; Hu, Z.; Zhu, Y. Polar Molecules Modified Perovskite Surface to Reduce the Recombination in Perovskite Solar Cells. *RSC Adv.* **2015**, *6*, 9090−9095.

(33) Xu, J.; Buin, A.; Ip, A. H.; Li, W.; Voznyy, O.; Comin, R.; Yuan, M.; Jeon, S.; Ning, Z.; McDowell, J. J.; et al. Perovskite−fullerene Hybrid Materials Suppress Hysteresis in Planar Diodes. *Nat. Commun.* **2015**, *6*, 7081.

(34) Shao, Y.; Xiao, Z.; Bi, C.; Yuan, Y.; Huang, J. Origin and Elimination of Photocurrent Hysteresis by Fullerene Passivation in $CH_3NH_3PbI_3$ Planar Heterojunction Solar Cells. *Nat. Commun.* **2014**, *5*, 5784.

(35) Liang, P.-W.; Chueh, C.-C.; Williams, S. T.; Jen, A. K.-Y. Roles of Fullerene-Based Interlayers in Enhancing the Performance of Organometal Perovskite Thin-Film Solar Cells. *Adv. Energy Mater.* **2015**, *5*, 1402321.

(36) Li, C. Z.; Chueh, C. C.; Yip, H. L.; Ding, F.; Li, X.; Jen, A. K. Y. *Adv. Mater.* **2013**, *25*, 2457−2461.

(37) Li, C. Z.; Chueh, C. C.; Ding, F.; Yip, H. L.; Liang, P. W.; Li, X.; Jen, A. K. Y. *Adv. Mater.* **2013**, *25*, 4425−4430.

(38) Dohner, E. R.; Jaffe, A.; Bradshaw, L. R.; Karunadasa, H. I. Intrinsic White-Light Emission from Layered Hybrid Perovskites. *J. Am. Chem. Soc.* **2014**, *136*, 13154−13157.

(39) Lemmerer, A.; Billing, D. G. Lead Halide Inorganic−organic Hybrids Incorporating Diammonium Cations. *CrystEngComm* **2012**, *14*, 1954.

(40) Yang, S.; Zheng, Y. C.; Hou, Y.; Chen, X.; Chen, Y.; Wang, Y.; Zhao, H.; Yang, H. G. Formation Mechanism of Freestanding $CH_3NH_3PbI_3$ Functional Crystals: In Situ Transformation vs Dissolution−Crystallization. *Chem. Mater.* **2014**, *26*, 6705−6710.

(41) Quan, L. N.; Yuan, M.; Comin, R.; Voznyy, O.; Beauregard, E. M.; Hoogland, S.; Buin, A.; Kirmani, A. R.; Zhao, K.; Amassian, A.; et al. Ligand-Stabilized Reduced-Dimensionality Perovskites. *J. Am. Chem. Soc.* **2016**, *138*, 2649−2655.

(42) Smith, I. C.; Hoke, E. T.; Solis-Ibarra, D.; McGehee, M. D.; Karunadasa, H. I. A Layered Hybrid Perovskite Solar-Cell Absorber with Enhanced Moisture Stability. *Angew. Chem., Int. Ed.* **2014**, *53*, 11232−11235.

(43) Cao, D. H.; Stoumpos, C. C.; Farha, O. K.; Hupp, J. T.; Kanatzidis, M. G. Two-Dimensional Homologous Perovskites as Light Absorbing Materials for Solar Cell Applications. *J. Am. Chem. Soc.* **2015**, *137* (24), 7843−7850.

(44) Zhang, Y.-Y.; Chen, S.; Xu, P.; Xiang, H.; Gong, X.-G.; Walsh, A.; Wei, S. Intrinsic Instability of the Hybrid Halide Perovskite Semiconductor $CH_3NH_3PbI_3$. arXiv:1506.01301. http://arxiv.org/abs/1506.01301.

(45) He, Z.; Zhong, C.; Huang, X.; Wong, W. Y.; Wu, H.; Chen, L.; Su, S.; Cao, Y. Simultaneous Enhancement of Open-Circuit Voltage, Short-Circuit Current Density, and Fill Factor in Polymer Solar Cells. *Adv. Mater.* **2011**, *23*, 4636−4643.

(46) Chen, Q.; Mao, L.; Li, Y.; Kong, T.; Wu, N.; Ma, C.; Bai, S.; Jin, Y.; Wu, D.; Lu, W.; et al. Quantitative Operando Visualization of the Energy Band Depth Profile in Solar Cells. *Nat. Commun.* **2015**, *6*, 7745.

(47) Zhou, H.; Zhang, Y.; Seifter, J.; Collins, S. D.; Luo, C.; Bazan, G. C.; Nguyen, T. Q.; Heeger, A. J. High-Efficiency Polymer Solar Cells Enhanced by Solvent Treatment. *Adv. Mater.* **2013**, *25*, 1646−1652.

(48) Cowan, S. R.; Roy, a; Heeger, a J. Recombination in Polymer-Fullerene Bulk Heterojunction Solar Cells. *Phys. Rev. B: Condens. Matter Mater. Phys.* **2010**, *82*, 245207.

(49) Li, C. Z.; Chang, C. Y.; Zang, Y.; Ju, H. X.; Chueh, C. C.; Liang, P. W.; Cho, N.; Ginger, D. S.; Jen, A. K. Y. Suppressed Charge Recombination in Inverted Organic Photovoltaics via Enhanced Charge Extraction by Using a Conductive Fullerene Electron Transport Layer. *Adv. Mater.* **2014**, *26*, 6262−6267.

DOI: 10.1021/acsenergylett.6b00327
ACS Energy Lett. 2016, 1, 757−763